Crystal Structures of Ni^{2+}- and Tl^{+}-Exchanged Zeolite X, $Ni_{17}Tl_{58}Si_{100}Al_{92}O_{384}$ and $Ni_{12}Tl_{68}Si_{100}Al_{92}O_{384}$

Mee Kyung Song, Bo young Yoon, and Yang Kim*

Department of Chemistry and Chemistry Institute for Functional Materials, Pusan National University, Pusan 609-735, Korea
Received October 4, 2000

The crystal structures of fully dehydrated Ni^{2+}- and Tl^{+}-exchanged zeolite X ($Ni_{17}Tl_{58}$-X, and $Ni_{12}Tl_{68}$-X; X=$Si_{100}Al_{92}O_{384}$) have been determined by single-crystal X-ray diffraction techniques in the cubic space group $Fd\bar{3}$ at 21(1)°C (a=24.380(4) Å, 24.660(4) Å, respectively). Their structures have been refined to the final error indices R_1=0.037 and R_2=0.043 with 485 reflections, and R_1=0.039 and R_2=0.040 with 306 reflections, respectively, for which $I>3\sigma(I)$. In $Ni_{17}Tl_{58}$-X, 17 Ni^{2+} ions per unit cell were found at only two sites: 15 at site I at the center of the hexagonal prism (Ni-O=2.203(9) Å) and the remaining 2 at site II near single six-oxygen rings in the supercage (Ni-O=2.16(3) Å). Fifty-eight Tl^{+} ions were found at five crystallographic sites: 28 at site II (Tl-O=2.626(8) Å), 2 at site I′ in the sodalite cavity near the hexagonal prism (Tl-O=2.85(1) Å), another 2 at site II′ in the sodalite cavity (Tl-O=2.77(1) Å). The remaining 26 were found at two nonequivalent III′ sites with occupancies of 23 and 3. In $Ni_{12}Tl_{68}$-X, 12 Ni^{2+} ions per unit cell were found at two sites: 10 at site I (Ni-O=2.37(2) Å) and the remaining 2 at site II (Ni-O=2.13(2) Å). Sixty-eight Tl^{+} ions were found at five crystallographic sites: 28 at site II (Tl-O=2.63(1) Å), 12 at site I′ (Tl-O=2.62(1) Å), 2 at site II′ (Tl-O=3.01(2) Å), and the remaining 26 at two III′ sites with occupancies of 23 and 3. It appears that Ni^{2+} ions prefer to occupy site I and II, in that order. The large Tl^{+} ions occupy the remaining sites, I′, II, II′ and two different III′ sites. In both crystals, only the Ni^{2+} ions at site II were reduced and migrated to the external surface of zeolite X when these crystals were treated with hydrogen gas.

Keywords : Structure, Zeolite X, Nickel, Thallium, Ion-exchange.

Introduction

Dispersed nickel supported on various oxides has been used as a catalyst in the hydrogenation, dehydrogenation, and hydrogenolysis reactions.[1-3] The support has multiple effects on the formation of metal particles and on the catalytic reactions. It is available to stabilize the nickel in a dispersed state and inhibit its sintering. It can also provide acidic sites and play a role in dual functional catalysts.[4-5] Actually, zeolites contain cavities with well defined size and strong acidic sites.[6-8] Metal particles can be entrapped within the cavities and some catalytic reactions that are catalyzed by metals occur.

Several studies concerning the formation and catalytic properties of nickel metal in A, X and Y type zeolites are reported.[9-11] By treating a zeolite containing Ni^{2+} ions or nickel complex cations with hydrogen at elevated temperature, the major part of the nickel is reduced to metallic nickel, which partially migrates and agglomerates on the zeolite surface as crystallites and partially remains in the intracrystalline structure in the form of clusters.[12] The formation of clusters can be verified using the change of the unit cell parameters taking place during Ni^{2+} reduction.

Investigations into reduced nickel faujasite catalysts show that the reducibility and the resulting catalytic activity depend on the location of Ni^{2+} ions, the nature and concentration of other elements, and the pretreatment and reduction conditions. The reducibility of Ni^{2+} ions also depends on the composition and redox properties of the zeolite framework. It is known that the Ni^{2+} ion is more reducible in framework A than in X and Y zeolites.[13]

The distributions of cations in faujasite-type zeolites have been widely studied by X-ray diffraction method.[14-15] Several structural studies of mixed cation systems of monovalent and divalent ion exchanged zeolite A and X also have been reported to investigate the site selectivity of various cations.[16-20] It has been observed that the small and highly charged Cd^{2+}, Ca^{2+} and Sr^{2+} ions prefer to occupy site I, with the remainder going to site II. The large Tl^{+}, Cs^{+}, and Rb^{+} ions, which are less able to balance the anionic charge of the zeolite framework than the small and highly charged divalent ions, fill site I and finish filling site II with the remainder going to the least suitable cationic sites in the structure, sites III and III′.

The present work was done to study the relative positions of cations in fully dehydrated Ni^{2+}- and Tl^{+}-exchanged zeolite X. As the structural stability and catalytic property of zeolites depend on the type and number of cations and their distribution over the available sites, it is meaningful to determine the cationic positions and occupancies in the zeolite framework. The effect of treating Ni^{2+} ions with H_2 in zeolite X was also studied here.

*To whom all the correspondence should be addressed. Fax: +82-51-516-7421, e-mail: ykim@hyowon.pusan.ac.kr

Experimental Section

Large single crystals of sodium zeolite X, $Na_{92}Si_{100}Al_{92}O_{384}$, were prepared in St. Petersburg, Russia.[21] Each of two single crystals, octahedron with a cross-section of about 0.2 mm, was lodged in a fine Pyrex capillary for ion exchange. $Ni_{17}Tl_{58}$-X and $Ni_{12}Tl_{68}$-X were prepared using an exchange solution whose $Ni(NO_3)_2{\cdot}6H_2O$: $TlNO_3$ mole ratio was 10 : 1 and 1 : 1, with a total concentration of 0.05 M. The solution was allowed to flow past the crystal at a velocity of approximately 15 mm/s for 4 days at 21(1) °C. The crystals were dehydrated at 360 °C under 2×10^{-6} Torr for 2 days. The color of crystals was black. Two other crystals were prepared by the same method and treated with 100 Torr of H_2 for 1 hour at 21(1) °C to reduce Ni^{2+} ions and to form Ni clusters within the zeolite cavities. Then, each crystal was evacuated at room temperature and 2×10^{-6} Torr for 2 hours. Each crystal was sealed in a Pyrex capillary by a torch.

The cubic space group $Fd\bar{3}$ was used throughout this work. It was justified by the low Si/Al ratio, which in turn requires, at least in the short range, the alternation of Si and Al, and by the observation that this crystal, like all other crystals from the same batch, does not have intensity with symmetry across (110) and, therefore, lacks that mirror plane. Diffraction data were collected with an automated four-circle CAD-4 diffractometer equipped with a pulse-height analyzer and graphite monochromator. Molybdebum radiation was used for all experiments ($K\alpha_1$, λ=0.70930 Å; $K\alpha_2$, λ=0.71359 Å). The cubic unit cell constant, a, determined by a least-squares refinement of 25 intense reflections for which $14° < 2\theta < 22°$ at 21(1) °C are 24.380(4) Å and 24.660(4) Å for $Ni_{17}Tl_{58}$-X and $Ni_{12}Tl_{68}$-X, respectively. All unique reflections in the positive octant of an F-centered unit cell for which $2\theta < 50°$, $l > h$, and $k > h$, were recorded. Of the 1327 unique reflections measured for $Ni_{17}Tl_{58}$-X and the 1344 for $Ni_{12}Tl_{68}$-X, only 485 and 306 reflections, respectively, for which $I > 3\sigma(I)$ were used in subsequent structure determination. Spherical absorption corrections (for $Ni_{17}Tl_{58}$-X crystal, μR=1.93 and d_{cal}=2.781 g/cm^3; for $Ni_{12}Tl_{68}$-X crystal, μR=1.87 and d_{cal}=2.881 g/cm^3) were applied.[22] The calculated transmission coefficients ranged from 0.08 to 0.10 for both crystals. These corrections had little effect on the final R indices. The summary of data collection as well as the crystal structure determination are presented in Table 1.

Table 1. Crystallographic Data

		$Ni_{17}Tl_{58}$-X	$Ni_{12}Tl_{68}$-X
Space group		$Fd\bar{3}$	$Fd\bar{3}$
Unit cell constant, a (Å)		24.380(4)	24.660(4)
d_{calcd} (g/cm^3)		2.781	2.881
Diffractometer		Enraf-Nonius CAD-4	Enraf-Nonius CAD-4
Data collection temperature (°C)		21	21
Radiation (Mo K_α)	λ_1(Å)	0.70930	0.70930
	λ_2(Å)	0.71359	0.71359
Number of reflections gathered		1327	1344
Number of reflections ($I > 3\sigma(I)$)		485	306
Final R indices($I > 3\sigma(I)$)	R_1[a]	0.037	0.039
	wR_2[b]	0.043	0.040

[a] $R_1 = (\Sigma(|F_o| - |F_c|)/\Sigma F_o)$. [b] $wR_2 = (\Sigma w(|F_o| - |F_c|)^2/\Sigma wF_o^2)^{1/2}$.

Structure Determination

$Ni_{17}Tl_{58}$-X. The full-matrix least-squares refinement was initiated by using the atomic parameters of the framework atoms [Si, Al, O(1), O(2), O(3), and O(4)] in dehydrated $Ca_{18}Tl_{56}$-X.[23] The anisotropic refinement converged to an unweighted R_1 index. ($\Sigma(|F_o| - |F_c|)/\Sigma F_o$), of 0.61 and a weighted R_2 (wR_2) index. $(\Sigma w(|F_o| - |F_c|)^2/\Sigma wF_o^2)^{1/2}$, of 0.69.

A difference Fourier function revealed two large peaks at (0.257, 0.257, 0.257) and (0.0, 0.0, 0.0), with heights of 24.2 eÅ^{-3} and 9.98 eÅ^{-3}, respectively. The anisotropic refinement, including these peaks as Tl^+ ions at Tl(2) and Ni^{2+} ions at Ni(1), converged to R_1=0.24 and wR_2=0.37, with occupancies of 27.4(1) and 14.9(2), respectively. These values were reset and fixed at 28 Tl^+ and 15 Ni^{2+} ions, respectively.

Distinguish Ni^{2+} from Tl^+ ions is easy for several reasons. First, their atomic scattering factors are quite different (26 e$^-$ for Ni^{2+} and 80 e$^-$ for Tl^+). Secondly, their ionic radii are different (Ni^{2+}=0.69 and Tl^+=1.47 Å).[24] Also, the approach distances between Tl^+ ions and oxygens in zeolite framework in dehydrated Tl_{92}-X[25] have been determined and are indicative.

A subsequent difference Fourier synthesis revealed two additional peaks, at Tl(3): (0.41, 0.11, 0.13), with a height of 20.9 eÅ^{-3}, and at Tl(5): (0.177, 0.177, 0.177), with a height of 11.0 eÅ^{-3}. Inclusion of these peaks as ions at Tl(3) and Tl(5) lowered the error indices to R_1=0.058 and wR_2=0.069. The occupancy numbers at Tl(3) and Tl(5) were refined to 24.1(2) and 2.4(2), respectively. On ensuring the difference Fourier function, two peaks appeared, at Tl(1): (0.08, 0.08, 0.08), with a peak height of 4.69 eÅ^{-3}, and at Tl(4): (0.41, 0.08, 0.08), with a height of 5.3 eÅ^{-3}. The anisotropic refinement, including these Tl^+ ions, Tl(1) and Tl(4), converged to R_1=0.044 and wR_2=0.055. From successive difference Fouriers, one peak was found at Ni(2), (0.22, 0.22, 0.22), with a height of 2.5 eÅ^{-3}. This peak was stable in least-squares refinement. The anisotropic refinement of framework atoms and all cations, except Ni(2) and Tl(4), which were refined isotropically, converged to R_1=0.037 and wR_2=0.042. The anisotropic refinements of Ni(2) and Tl(4) gave negative values of the thermal ellipsoids, which were physically unacceptable. The occupancies of Ni(1), Ni(2), Tl(1), Tl(2), Tl(3), Tl(4), and Tl(5) were fixed at the values shown in Table 2(a), considering the cationic charge per unit cell. The final error indices for the 485 reflections for which $I > 3\sigma(I)$ were R_1=0.037 and wR_2=0.043.

$Ni_{12}Tl_{68}$-X. The full-matrix least-squares refinement was initiated by using the atomic parameters of the framework atoms for the previous crystal of $Ni_{17}Tl_{58}$-X. The anisotropic refinement converged to R_1=0.61 and wR_2=0.69. A difference Fourier function revealed a peak at (0.253, 0.253, 0.253) with a height of 22.3 eÅ^{-3}. The anisotropic refine-

Table 2. Positional, thermal, and occupancy parameters[a]

(a) $Ni_{17}Tl_{58}$-X

Atom	Wyc. Pos.	*x*	*y*	*z*	[b]U_{11} or [d]U_{iso}	U_{22}	U_{33}	U_{12}	U_{13}	U_{23}	[c]Occupancy	
											varied	fixed
Si	96(g)	−524(2)	1226(2)	332(2)	106(17)	102(17)	120(19)	−26(18)	−22(16)	−20(18)		96
Al	96(g)	−532(2)	375(2)	1210(2)	109(18)	88(19)	53(18)	2(17)	−11(18)	−44(19)		96
O(1)	96(g)	−1108(4)	25(4)	1076(4)	266(57)	354(59)	271(54)	−135(58)	146(43)	−198(57)		96
O(2)	96(g)	−35(5)	−34(4)	1475(4)	339(51)	250(47)	108(41)	160(50)	−57(54)	−33(52)		96
O(3)	96(g)	−318(4)	620(4)	576(4)	191(55)	131(51)	166(53)	−16(47)	−34(50)	−3(44)		96
O(4)	96(g)	−668(4)	855(4)	1681(4)	246(56)	162(53)	145(51)	42(48)	53(48)	8(45)		96
Ni(1)	16(c)	0	0	0	123(8)	123(8)	123(8)	3(13)	3(13)	3(13)	14.9(2)	15
Ni(2)	32(e)	2294(37)	2294(37)	2294(37)	476(415)						1.9(1)	2
Tl(1)	32(e)	811(8)	811(8)	811(8)	684(79)	684(79)	684(79)	101(96)	101(96)	101(96)	1.7(1)	2
Tl(2)	32(e)	2552(1)	2552(1)	2552(1)	252(2)	252(2)	252(2)	−26(4)	−26(4)	−26(4)	27.4(1)	28
Tl(3)	96(g)	4129(1)	1176(2)	1382(2)	150(11)	1034(28)	945(38)	−130(21)	151(16)	88(27)	24.1(2)	23
Tl(4)	96(g)	4180(16)	893(17)	871(17)	851(96)						3.3(2)	3
Tl(5)	32(e)	1755(3)	1755(3)	1755(3)	180(26)	180(26)	180(26)	52(30)	52(30)	52(30)	2.4(2)	2

(b) $Ni_{12}Tl_{68}$−X

Atom	Wyc. Pos.	*x*	*y*	*z*	[b]U_{11} or [d]U_{iso}	U_{22}	U_{33}	U_{12}	U_{13}	U_{23}	[c]Occupancy	
											varied	fixed
Si	96(g)	−523(3)	356(3)	1231(3)	218(33)	136(33)	228(32)	−9(31)	22(36)	−58(34)		96
Al	96(g)	−524(3)	1227(3)	362(3)	177(34)	149(33)	160(36)	58(36)	20(32)	−62(35)		96
O(1)	96(g)	−1068(7)	−11(8)	1079(6)	539(114)	502(108)	258(117)	−264(117)	−13(76)	109(108)		96
O(2)	96(g)	−29(8)	−21(8)	1481(5)	411(85)	339(79)	270(73)	58(104)	−33(105)	47(103)		96
O(3)	96(g)	−299(6)	634(6)	657(7)	323(102)	260(98)	344(105)	53(92)	68(89)	144(87)		96
O(4)	96(g)	−694(6)	800(6)	1708(7)	125(89)	271(95)	381(101)	−91(84)	−103(91)	−117(80)		96
Ni(1)	16(c)	0	0	0	123(19)	123(19)	123(19)	96(36)	96(36)	96(36)	10.7(2)	10
Ni(2)	32(e)	2261(18)	2261(18)	2261(18)	14(160)						1.9(3)	2
Tl(1)	32(e)	754(1)	754(1)	754(1)	341(13)	341(13)	341(13)	22(16)	22(16)	22(16)	13.0(2)	12
Tl(2)	32(e)	2546(1)	2546(1)	2546(1)	319(4)	319(4)	319(4)	−16(7)	−16(7)	−16(7)	27.9(1)	28
Tl(3)	96(g)	4135(2)	1114(3)	1377(3)	231(24)	1209(65)	1170(63)	−260(34)	235(34)	−131(39)	22.6(2)	23
Tl(4)	96(g)	4155(27)	853(29)	851(29)	1096(169)						2.6(2)	3
Tl(5)	32(e)	1673(28)	1673(28)	1673(28)	2826(528)	2826(528)	2826(528)	−306(494)	−306(494)	−306(494)	1.7(2)	2

[a]Positional and anisotropic thermal parameters are given × 10^4. Numbers in parentheses are the esds in the units of the least significant digit given for the corresponding parameter. [b]The anisotropic temperature factor = $\exp[(-2\pi^2/a^2)(U_{11}h^2+U_{22}k^2+U_{33}l^2+U_{12}hk+U_{13}hl+U_{23}kl)]$. [c]Occupancy factors are given as the number of atoms or ions per unit cell. [d]$U_{iso}=(B_{iso}/8\pi^2)$

ment, including this as Tl^+ ion at Tl(2), converged to R_1=0.32 and wR_2=0.43, with an occupancy of 27.9(1).

A subsequent difference Fourier function revealed two additional peaks, one at (0, 0, 0), with a height of 23.9 eÅ^{-3} and the other at (0.08, 0.08, 0.08), with a height of 16.9 eÅ^{-3}. Inclusion of these peaks as ions at Ni(1) and Tl(1) lowered the error indices to R_1=0.18 and wR_2=0.31. The occupancy numbers at Ni(1) and Tl(1) were refined to 10.7(2) and 13.0(2), respectively. On ensuring the Fourier functions, three peaks appeared, at Tl(3): (0.40, 0.12, 0.12), with a height of 13.4 eÅ^{-3}, at Tl(5): (0.179, 0.179, 0.179), with a height of 3.65 eÅ^{-3}, and at Tl(4): (0.41, 0.09, 0.09), with a height of 1.56 eÅ^{-3}. From successive difference Fouriers, one peak was found at (0.22, 0.22, 0.22), Ni(2), with a height of 1.4 eÅ^{-3}. These peaks were stable in least-squares refinement.

The anisotropic refinement of framework atoms and all the cations, except Ni(2) and Tl(4), which were refined isotropically, converged to R_1=0.045 and wR_2=0.043. The occupancies of Ni(1), Ni(2), Tl(1), Tl(2), Tl(3), Tl(4), and Tl(5) were fixed at the values shown in the Table 2(b), considering the cationic charge per unit cell. The sum of the occupancy numbers at Ni(2), Tl(2), and Tl(5) were fixed at 32.0, which is the maximum number of ions per unit cell at these positions. The final error indices for the 306 reflections for which $I>3\sigma(I)$ were R_1=0.039 and wR_2=0.040.

The shifts in the final cycle of least-squares refinements were less than 0.1% of their corresponding standard deviations for both crystals. All crystallographic calculations were done using MolEN.[26] Atomic scattering factors[27] for Si, Al, O^-, Ni^{2+}, and Tl^+ were used. All scattering factors were modified to account for anomalous dispersion.[28,29] The final structural parameters are given in Table 2 and selected interatomic distances and angles are in Table 3.

Table 3. Selected interatomic distances (Å) and angles (deg)[a]

	Ni_7Tl_{58}-X	$Ni_{12}Tl_{68}$-X
Si-O(1)	1.63(1)	1.66(2)
Si-O(2)	1.61(1)	1.65(2)
Si-O(3)	1.67(1)	1.67(2)
Si-O(4)	1.61(1)	1.66(2)
Average	**1.63**	**1.66**
Al-O(1)	1.68(1)	1.67(2)
Al-O(2)	1.70(1)	1.69(2)
Al-O(3)	1.74(1)	1.73(2)
Al-O(4)	1.67(1)	1.63(2)
Average	**1.70**	**1.68**
Ni(1)-O(3)	2.203(9)	2.37(2)
Ni(2)-O(2)	2.16(3)	2.13(2)
Tl(1)-O(3)	2.85(1)	2.62(1)
Tl(2)-O(2)	2.626(8)	2.63(1)
Tl(3)-O(4)	2.71(1)/2.82(1)	2.84(2)
Tl(4)-O(1)	2.87(4)/2.90(4)	2.93(7)
Tl(5)-O(2)	2.77(1)	3.01(2)
O(1)-Si-O(2)	112.4(6)	112.0(1)
O(1)-Si-O(3)	106.4(5)	107.5(8)
O(1)-Si-O(4)	109.1(5)	108.4(8)
O(2)-Si-O(3)	107.9(5)	107.6(8)
O(2)-Si-O(4)	109.5(5)	106.9(8)
O(3)-Si-O(4)	111.4(5)	114.6(9)
O(1)-Al-O(2)	112.0(6)	113.0(1)
O(1)-Al-O(3)	108.7(4)	106.5(9)
O(1)-Al-O(4)	109.9(4)	107.1(9)
O(2)-Al-O(3)	109.1(5)	108.6(8)
O(2)-Al-O(4)	107.0(5)	107.1(8)
O(3)-Al-O(4)	114.7(3)	114.5(9)
Si-O(1)-Al	125.6(6)	131.0(1)
Si-O(2)-Al	133.5(6)	134.0(9)
Si-O(3)-Al	126.9(3)	127.0(1)
Si-O(4)-Al	155.3(7)	150.0(1)
O(3)-Ni(1)-O(3)	88.4(3)/91.6(3)/180[b]	88.1(5)/91.9(5)/180[b]
O(2)-Ni(2)-O(2)	115.0(2)	117.0(2)
O(3)-Tl(1)-O(3)	67.3(4)	77.7(5)
O(2)-Tl(2)-O(2)	88.1(3)	87.7(6)
O(4)-Tl(3)-O(4)	62.0(3)	67.6(4)
O(1)-Tl(4)-O(1)	115.0(1)	117.0(2)
O(1)-Tl(4)-O(4)	58.1(9)/60.8(9)	60.0(2)
O(2)-Tl(5)-O(2)	82.4(3)	74.5(7)

[a]Numbers in parentheses are estimated standard deviations in least significant digit given for the corresponding values. [b]Exactly by symmetry.

Discussion

Zeolite X is a synthetic version of the mineral faujasite, having opened, negatively charged frameworks. The 14-hedron with 24 vertices, known as the sodalite cavity or β-cage, may be viewed as the principal building block of the aluminosilicate framework of the zeolite (see Figure 1). These β-cages are connected tetrahedrally at six-rings by bridging oxygen to give double six-ring (D6R, hexagonal prisms) and, concomitantly, to give an interconnected set of

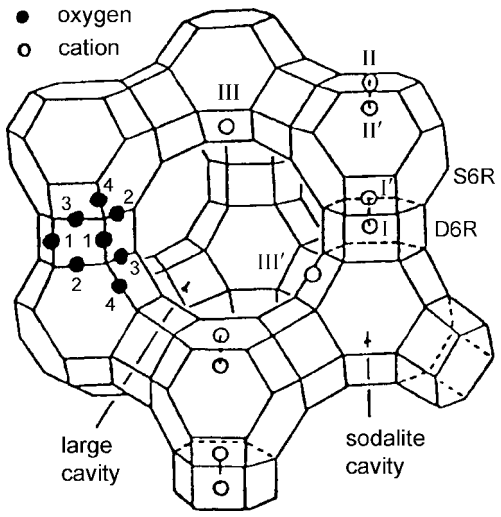

Figure 1. A stylized drawing of the framework structure of zeolite X. Near the center of each line segment is an oxygen atom. The numbers from 1 to 4 indicates the four different oxygen atoms. Silicon and aluminum atoms alternate at the tetrahedral intersections, except that a silicon atom substitutes for aluminum at about 4 % of the Al positions. Extraframework cation positions are labeled with Roman numerals.

even larger cavities (supercages) accessible in three dimensions through 12-ring (24-membered) windows. The Si and Al atoms occupy the vertices of this polyhedral. The oxygen atoms lie approximately midway between each pair of Si and Al atoms, but are displaced from those points to give near tetrahedral angles about Si and Al.

Exchangeable cations that balance the negative charge of the aluminosilicate framework are found within the zeolite's cavities. They are usually found at the following sites shown in Figure 1 : site I at the center of a D6R; I′ in the sodalite cavity on the opposite side of one of the D6R from site I; II′ inside the sodalite cavity near a single six-ring (S6R) entrance to the supercage; II in the supercage adjacent to a S6R; III in the supercage opposite a four-ring between two 12-rings; and III' in the vicinity of III but off the twofold axis.[30,31]

Ni_7Tl_{58}-X. The mean values of the Si-O and Al-O bond lengths are normal, *ca.* 1.63 Å and 1.70 Å, respectively. The individual bond lengths, however, show marked variations: Si-O from 1.61(1) Å to 1.67(1) Å, and Al-O from 1.67(1) Å to 1.74(1) Å. The Si-O and Al-O distances depend on the positions and coordination of cations to framework oxygen (see Table 3).

In this structure, 17 Ni^{2+} ions occupy two crystallographic sites and 58 Tl^{+} ions occupy five different sites. 15 Ni^{2+} ions at Ni(1) fill the octahedral site I (see Figures 2 and 3). The octahedral Ni(1)-O(3) distance of 2.203(9) Å is a little longer than the sum of the ionic radii of Ni^{2+} and O^{2-} (0.69+1.32=2.01 Å)[24] but is nearly the same as the bond distance in natural faujasite (Ni^{2+}-O(3)=2.289 Å).[32] The remaining 2 Ni^{2+} ions at Ni(2) are at site II in the supercage (see Figure 2). The bond distance of Ni(2)-O(2) is 2.16(3) Å.

As every site I is surrounded by two I′ sites, the neighbor-

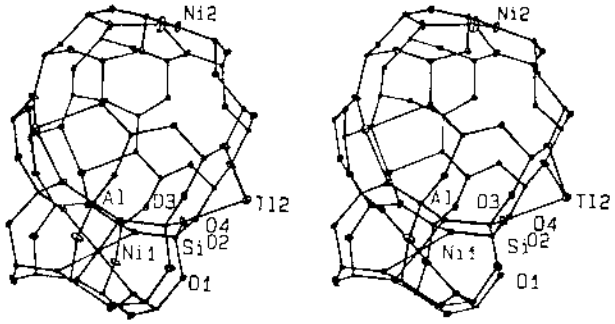

Figure 2. Stereoview of a sodalite cavity with an attached D6R in dehydrated $Ni_{12}Tl_{68}$-X. One Ni^{2+} ion at Ni(1) (site I), three Tl^{+} ions at Tl(2) (site II), and one Ni^{2+} ion at Ni(2) (site II) are shown. About 25% of sodalite cavities may have this arrangement. Ellipsoids of 20% probability are shown.

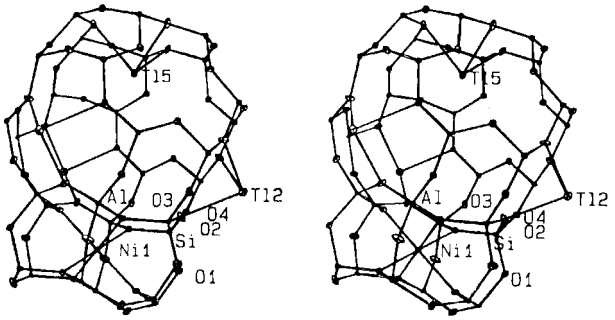

Figure 3. Stereoview of a sodalite cavity with an attached D6R in dehydrated $Ni_{12}Tl_{68}$-X. One Ni^{2+} ion at Ni(1) (site I), three Tl^{+} ions at Tl(2) (site II), and one Tl^{-} ion at Tl(5) (site II′) are shown. About 25% of sodalite cavities may have this arrangement. Ellipsoids of 20% probability are shown.

ing positions I and I′ cannot be occupied simultaneously because of the strong electrostatic repulsion between ions. Thus, the respective site occupation of $n(1)+n(1')/2$ should be less than and equal to 16 where $n(1)$ and $n(1')$ are the numbers of cations in each site per unit cell. From this relationship, the observed cation populations of the remaining I′ sites are equal to 2. The 2 I′ sites are filled by Tl^{-} ions at Tl(1). The Tl(1)-O(3) bond distance is 2.85(1) Å, which is almost the same as the sum of the ionic radii of Tl^{+} and O^{2-} (1.47+1.32=2.79 Å).[24] Tl^{+} ions at Tl(1) form ionic bonds with three framework oxygens, O(3).

About 28 Tl^{-} ions at Tl(2) occupy the 32-fold site II in the supercage. The Tl(2)-O(2) Å bond distance is 2.626(8) Å, which is a little shorter than the sum of the corresponding ionic radii, 2.79 Å.[24] Each Tl(2) ion is recessed 1.76(1) Å from the plane of three O(2) oxygens of the single six ring. About 50% of the supercages have the maximum 4 Tl^{-} ions at Tl(2) in the supercage. The 4 Tl^{-} ions in the supercage that are in the tetrahedral position by themselves may have a large electrostatic repulsion between them. To compensate for the large electrostatic repulsion and stabilize their structures, Tl^{+} ions at Tl(2) push each other to the charged oxygen plane, which results in the slightly shorter distance of the Tl(2)-O(2) bond.

The 2 Tl^{-} ions occupy the 32-fold Tl(5) positions at site II′

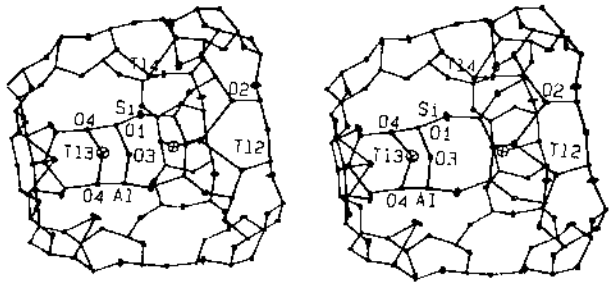

Figure 4. Stereoview of the supercage of dehydrated $Ni_{12}Tl_{68}$-X. Three Tl^{-} ions at Tl(2) (site II), three Tl^{-} ions at Tl(3) (site III′), and one Tl^{-} ion at Tl(4) (site III′) are shown. About 25% supercages may have this arrangement. Ellipsoids of 20% probability are used.

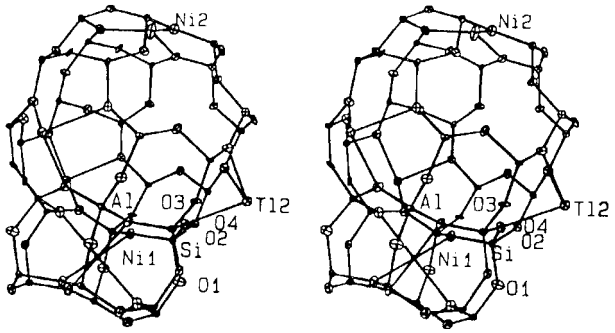

Figure 5. Stereoview of a sodalite cavity with an attached D6R in dehydrated $Ni_{12}Tl_{68}$-X. One Ni^{2+} ion at Ni(1) (site I), one Ni^{+} ion at Ni(2) (site II), and three Tl^{-} ions at Tl(2) (site II) are shown. About 25% of sodalite cavities may have this arrangement. Ellipsoids of 20% probability are shown.

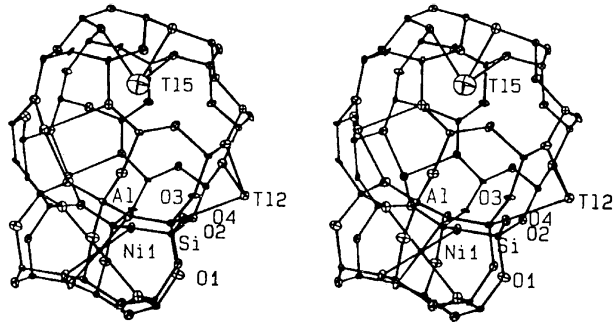

Figure 6. Stereoview of a sodalite cavity with an attached D6R in dehydrated $Ni_{12}Tl_{68}$-X. One Ni^{2+} ion at Ni(1) (site I), three Tl^{-} ions at Tl(2) (site II), and one Tl^{-} ion at Tl(5) (site II′) are shown. About 25% of sodalite cavities may have this arrangement. Ellipsoids of 20% probability are shown.

(see Figure 3). The remaining 26 Tl^{-} ions occupy crystallographically two different III′ sites at Tl(3) and Tl(4) in the supercage, with occupancies of 23 and 3, respectively(see Figure 4). The Tl(5)-O(2) Å bond distance, 2.77(1) Å, is nearly the same as the sum of the ionic radii of Tl^{-} and O^{2-}, 2.79 Å.

$Ni_{12}Tl_{68}$-X. In this structure, 12 Ni^{2+} ions occupy two crystallographic sites and 68 Tl^{-} ions occupy five different sites. 10 Ni^{2+} ions at Ni(1) fill the octahedral site I (see Figures 5 and 6). The octahedral Ni(1)-O(3) distance, 2.37(2) Å, is much longer than the sum of the ionic radii of Ni^{2+} and O^{2-}, 2.01 Å,[24] but is nearly the same as the bond distance

Table 4. Deviations (Å) of cations from six-ring planes

	$Ni_{17}Tl_{58}$-X	$Ni_{12}Tl_{68}$-X
At O(3)[a]		
Ni(1)	−0.60(1)	−0.83(1)
Tl(1)	2.35(1)	2.04(1)
At O(2)[b]		
Ni(2)	0.67(5)	0.50(2)
Tl(2)	1.76(1)	1.72(1)
Tl(5)	−1.61(2)	−2.01(4)

[a]The negative and positive deviations indicate that the atom lies in a D6R and in the sodalite cavity, respectively. [b]The positive and negative deviations indicate that the atom lies in the supercage and in the sodalite cavity, respectively.

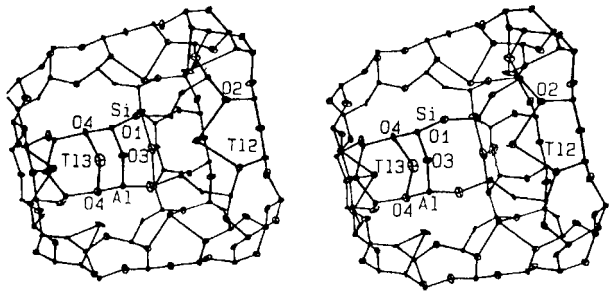

Figure 7. Stereoview of the supercage of dehydrated $Ni_{12}Tl_{68}$-X. Four Tl^+ ions at Tl(2) (site II) and three Tl^- ions Tl(3) (site III′) are shown. About 50% of the supercages may have this arrangement. Ellipsoids of 20% probability are used.

in natural faujasite, 2.289 Å.[32] The remaining 2 Ni^{2+} ions at Ni(2) are at site II in the supercage (see Figure 5). The bond distance of Ni(2)-O(2) is 2.13(2) Å. This Ni^{2-} ion is slightly recessed, 0.50 Å. into the supercage from the plane of three O(2) oxygen (see Tables 2 and 3). The O(2)-Ni(2)-O(2) bond angle, 117.0(2)°, is nearly trigonal planar.

12 Tl^+ ions at Tl(1) occupy the remaining 32-fold I′ sites. The Tl(1)-O(3) bond distance, 2.62(1) Å. is shorter than the sum of the ionic radii of Tl^- and O^{2-}, 2.79 Å.[24] About 2 Tl^+ ions at Tl(1) have electrostatic repulsion in each of the sodalite cavities. These ions push each other to the charged oxygen planes to get the stabilized positions in that cavity. This makes the bond distance of Tl(1)-O(3) shorter than the sum of the corresponding ionic radii. 28 Tl^+ ions at Tl(2) occupy site II far inside the supercage. Each Tl(2) ion is 1.72(1) Å from the plane of three O(2) oxygen of the S6R to which it is bound (see Table 4). The Tl(2)-O(2) distance is 2.63(1) Å. This distance is almost the same as in the $Ni_{17}Tl_{58}$-X. In this structure, about 50% of the supercages have four Tl^+ ions at Tl(2). The 4 Tl^+ ions at Tl(2) push each other to the charged oxygen planes to compensate for the large electrostatic repulsion and stabilize their structures. This results in a somewhat short bond distance of Tl(2)-O(2).

The Tl^- ions at Tl(3) and Tl(4) lie in the supercage at two crystallographically different III′ sites with occupancies of 23 and 3, respectively (see Figure 7). The remaining 2 Tl^+ ions at Tl(5) occupy the 32-fold position at site II′ (see Figure 5). They are recessed 2.01(4) Å into the sodalite cavities from the plane of three O(2) oxygen. Thus, the Tl(5)-O(2) bond distance. 3.01(2)Å. is somewhat longer than the sum of the ionic radii of Tl^- and O^{2-}, 2.79 Å.

Table 5. Distribution of nonframework atoms over sites

Sites	Crystals			
	$Ni_{17}Tl_{58}$-X	$Ni_{15}H_4Tl_{58}$-X	$Ni_{12}Tl_{68}$-X	$Ni_{10}H_4Tl_{68}$-X
I	15Ni(1)	15Ni(1)	10Ni(1)	10Ni(1)
I′	2Tl(1)	2Tl(1)	11Tl(1)	11Tl(1)
II′	2Tl(5)	2Tl(5)	2Tl(5)	2Tl(5)
II	2Ni(2)	–	2Ni(2)	–
	28Tl(2)	28Tl(2)	28Tl(2)	28Tl(2)
III′	23Tl(3)	23Tl(3)	23Tl(3)	23Tl(3)
	3Tl(4)	3Tl(4)	3Tl(4)	3Tl(4)

To study the structure of Ni clusters in $Ni_{17}Tl_{58}$-X and $Ni_{12}Tl_{68}$-X. H_2 gas was treated to reduce Ni^{2+} ions in zeolite X. Upon treating the dehydrated $Ni_{17}Tl_{58}$-X and $Ni_{12}Tl_{68}$-X with 100 Torr of H_2 gas for one hour at 21(1)°C, only Ni^{2-} ions at site II were reduced and moved out from the zeolite structure. The results for the relative occupancies of nonframework atoms over sites are given in Table 5. To compensate for the negative charge of the zeolite framework induced by the reduction of Ni^{2+} ions. the protons were introduced into the zeolite framework as follows:

$$\begin{matrix} Z-O \\ \\ Z-O \end{matrix} \!\!\diagdown\!\!\diagup\!\! Ni^{2+} \;+\; H_2 \;\rightleftharpoons\; 2\,ZOH' \;+\; Ni^{\circ}$$

It may be concluded that Ni^{2+} ions at site II, which are tetrahedrally coordinated. are readily reduced. but the octahedrally coordinated Ni^{2+} ions at site I, crystallographically a very stable site, are not reduced under mild reducing conditions, for example, treating with H_2 gas for one hour at 21(1) °C.

Conclusion

The present study indicates that all of the Na^- ions in zeolite X can be replaced readily by Ni^{2-} and Tl^+ ions. The ionic size and charge govern the competition for site I for both structures. The small and highly charged Ni^{2+} ions nearly fill the site I, with the remainder going to site II, affirming that Ni^{2-} ions prefer to occupy site I. The large Tl^+ ions, which are less able to balance the anionic charge of the zeolite framework. occupy the remaining sodalite cavities with some occupancies at site I′. Sites II, II′, and III′ are occupied by Tl^- ions. In both structures, no Tl^- ions occupy site I. The Tl^- ion is apparently too large to occupy the center of the double 6-ring. When the Ni^{2+}- and Tl^+-exchanged zeolite X was treated with hydrogen gas, the Ni^{2-} ions at site II were readily reduced and migrated to the external surface of zeolite X.

Acknowledgment. This work was supported in part by the Korean Research Foundations made in the program year

of 2000. Project No. 2000-015-DP0190.

Supporting Information Available. Tables of calculated and observed structure factors (10 pages). The Supporting materials will be given upon your reguest to the correspondence author.

References

1. Van Meerteen, R. Z. C.; Coenen, J. W. E. *J. Catal.* **1977**, *46*, 13.
2. Martin, G. A. *J. Catal.* **1979**, *60*, 345.
3. Frennet, A.; Degols, L.; Lienard, G.; Crucg, F. *J. Catal.* **1978**, *55*, 150.
4. Vannice, M. A.; Garten, R. L. *J. Catal.* **1979**, *56*, 236.
5. Whyte, T. E. *Catal. Rev.* **1973**, *8*, 117.
6. Rabo, J. A. *Zeolite Chemistry; and Catalysis, ACS Monograph* No. 171, 1976.
7. Breck, D. W. *Zeolite Molecular Sieves*; Wiley Jones: New York, 1974.
8. Imelik, B.; Naccache, C.; Ben Taarit, Y.; Vedrine, J. C.; Coudurier, G.; Praliaud, H. *Studies in Surface Science and Catalysis*; Elsevier: 1980; Vol. 5.
9. Richardson, J. T. *J. Catal.* **1971**, *22*, 122.
10. Rieckert, L.; Bunsenges, Ber. *Phys. Chem.* **1969**, *73*, 331.
11. Penchev, V.; Davidova, N.; Kanazirev, V.; Minchev, H.; Neinska, Y. *Adv. Chem. Ser.* **1973**, *121*, 461.
12. Uytterhoeven, J. B. *Acta Physica et Chemica* **1978**, *24*, 534.
13. Egerton, T. A.; Vickerman, J. C. *J. Chem. Soc. Faraday Trans. I* **1973**, *69*, 39.
14. Schollnes, R.; Broddack, R.; Kuhlmann, B.; Nozel, P.; Herden, H. Z. *J. Phys. Chem.* (Leipzig) **1981**, *262*, 17.
15. Egerton, T. S.; Stone, F. S. *J. Chem. Soc. Faraday Trans. I* **1970**, *66*, 2364.
16. Jang, S. B.; Song, S. H.; Kim, Y. *J. Korean. Chem. Soc.* **1995**, *39*, 1.
17. Jang, S. B.; Kim, M. S.; Han, Y. W.; Kim, Y. *Bull. Korean Chem. Soc.* **1996**, *17*, 7.
18. Kwon, J. H.; Jang, S. B.; Kim, Y. *J. Phys. Chem.* **1996**, *100*, 13720.
19. Kim, M. J.; Kim, Y.; Seff, K. *Korean J. Crystallogra.* **1997**, *8*, 1.
20. Yeom, Y. H.; Jang, S. B.; Kim, Y.; Song, S. H.; Seff, K. *J. Phys. Chem. B* **1997**, *101*, 6914.
21. Bogomolov, V. N.; Petranovskii, V. P. *Zeolites* **1986**, *6*, 418.
22. *International Tables for X-ray Crystallography*; Kynoch Press: Birmingham, England, 1974; Vol. II, p 302.
23. Choi, E. Y.; Kim, Y. *J. Korean Chem. Soc.* **1999**, *43*, 384.
24. *Handbook of Chemistry and Physics*; 70th ed. The Chemical Rubber Co.: Cleveland, Ohio, 1989/1990; pp F-187.
25. Kim, Y.; Han, Y. W.; Seff, K. *Zeolites* **1997**, *18*, 325.
26. *MolEN*; a structure determination package supplied by Enraf-Nonius: Netherlands, 1990.
27. *International Tables for X-ray Crystallography*; Kynoch Press: Birmingham, England, 1974; Vol. IV, p 73.
28. Cromer, D. T. *Acta Crystallogr.* **1965**, *18*, 17.
29. reference 27, p 149.
30. Sun, T.; Seff, K.; Heo, N. H.; Petranovskii, V. P. *Science* **1993**, *259*, 495.
31. Sun, T.; Seff, K. *Chem. Rev.* **1994**, *94*, 859.
32. Olson, D. H. *J. Phys. Chem.* **1968**, *72*, 4366.